Simultaneous determination of Fe 3p spin-orbit and exchange splittings in photoemission

Di-Jing Huang*
Department of Physics, University of Texas, Austin, Texas 78712

D. M. Riffe
Department of Physics, Utah State University, Logan, Utah 84322-4415

J. L. Erskine
Department of Physics, University of Texas, Austin, Texas 78712
(Received 13 January 1995)

Spin-resolved core-level photoemission data from the 3p level of ultrathin Fe films [1.4–5.1 monolayers (ML)] epitaxially grown on W(110) have been obtained. A nonlinear least-squares analysis, based on a one-particle Hamiltonian that simultaneously includes core-valence exchange and core-hole spin-orbit interactions, is developed. It is first tested on Fe 2p magnetic circular dichroism (MCD) photoemission spectra and shown to successfully describe the MCD asymmetry data. The model is then used to analyze our thin-film 3p data. With increasing film thickness the spin-orbit splitting (0.67±0.02 eV) remains constant (as expected), the exchange splitting increases from 0±0.12 eV to 0.41±0.05 eV, the average Fe film magnetization ($=1.2\pm0.3\mu_B$ at 1.4 ML) increases, and the singularity index decreases. The analysis highlights the importance of simultaneously considering all relevant photoemission parameters in extracting meaningful values of the spin-orbit and exchange interactions.

I. INTRODUCTION

Core-level photoemission has long been utilized as an atom-specific probe of the local electronic structure in a variety of solids. Its application to the investigation of magnetic structure dates to the pioneering work of Fadley *et al.* on Mn and Fe ions.[1] Recently, with the advent of three spin-sensitive techniques—spin-polarized photoemission, magnetic circular dichroism (MCD) in photoemission, and magnetic linear dichroism (MLD) in photoemission—the core-level spectra of ferromagnetic metals such as Fe have come under increased scrutiny. One particular core level which has been widely investigated in the 3d ferromagnets is the 3p state. The 3p level has several photoemission parameters which are quite sensitive to the valence-band structure: (1) the exchange splitting Δ_{exc} of the core states by the polarized 3d valence electrons, (2) the spin-orbit (SO) splitting Δ_{SO} which is affected by the valence-charge screening of the nuclear charge, (3) the lifetime of the core hole which is dominated by Auger transitions involving two 3d electrons, and (4) the singularity index α which parametrizes the screening of the core hole by the valence band. For the highly studied 3d ferromagnet Fe there is little, if any, consensus on the values of these important parameters. E.g., reported values of the Fe 3p exchange splitting include 0.26,[2] <0.5,[3] 0.5,[4,5] 0.7,[6] 0.77,[7] 0.95±0.05,[8] and 1.11±0.05 eV,[9] while the SO splitting has been deduced to be 0.7 eV (Ref. 10) and 1.1±0.1 eV.[8] From several measurements[2,3,5] it has been concluded that a lifetime difference for majority and minority core holes[11] exists; however, values for majority (minority) lifetime widths range between 1.7 and 2.7 eV (1.0 and 1.4 eV).[2,3] Similarly, fitted singularity indices for bulk Fe have ranged from 0.2 (Ref. 7) to 0.44.[2]

Part of the difficulty in deducing these crucial parameters has been that the exchange and SO splittings of the 3p states are of roughly the same magnitude.[12] Indeed, in analyses of the lifetime width and singularity index the SO splitting has been altogether ignored.[2,3,5] Further, many of the reported exchange splittings simply reflect the peak separation of minority and majority spectra.[2–6] Only recently have there been attempts to include the SO splitting in the deduction of the exchange interaction.[8,9] However, in those analyses a realistic line shape was not used in the comparisons between experiment and theory. Clearly, a model which simultaneously includes all of these parameters would be immensely helpful in meaningful extraction of the relevant physical information from the photoemission spectra.

In this paper we present spin-resolved 3p photoemission data from thin, ferromagnet Fe films grown on W(110). We then outline a simple one-electron model which simultaneously incorporates the spin-orbit and exchange interactions. It is shown that the model successfully describes Fe 2p MCD spectra[13] where the spin-orbit splitting is an order of magnitude larger than the exchange interaction. The model is then applied to our 3p spin-polarized spectra in order to simultaneously extract the spin-orbit and exchange splittings along with the lifetime and singularity-index line-shape parameters. The importance of simultaneously considering all relevant parameters clearly emerges from the analysis. The model and analysis technique should be widely applicable to

0163-1829/95/51(21)/15170(10)/$06.00

spin-sensitive photoemission spectra from itinerant ferromagnets when final-state scattering effects (such as spin-orbit induced polarization[14]) can be neglected.

II. EXPERIMENTAL DETAILS

The experiments were performed on the U5 undulator beam line at the National Synchrotron Light Source at Brookhaven National Laboratory. Ultrathin $p(1\times1)$ Fe films were epitaxially grown on a highly aligned, 250 K W(110) substrate at a rate of 0.5 ML/min using an electron-beam pendant-drop evaporator in a base pressure of 2×10^{-10} Torr. Each sample was subsequently annealed to ~400 K in order to produce a well-ordered film[15] before cooling to the measurement temperature of ~150 K. The cleanliness and the structure were checked by photoemission and low-energy electron diffraction, respectively.

The Fe film thicknesses were determined from a quartz microbalance crystal monitor which was calibrated by the attenuation of the substrate $4f$ core-level photoemission intensity. Figure 1 plots the W $4f$ integrated intensity vs the crystal monitor signal. The straight-line linear fit to the log of the $4f$ intensity illustrates that the intensity decay is well described by an exponential. From the straight-line fit and an experimental inelastic mean free path (IMFP) of 3.6 Å (Ref. 16) the absolute thicknesses of the films were determined. The uncertainty in film thicknesses arises largely from the ±20% uncertainty in the IMFP.[16]

Figure 2 illustrates the experimental geometry. *P*-polarized light (photon energy=93 eV) incident at an angle of 58.5° was used to excite the photoelectrons. The plane of incidence was defined by the [001] and [110] directions of the substrate. The Fe films were magnetized along either the $[1\bar{1}0]$ or $[\bar{1}10]$ directions by applying current pulses through a pair of Helmholtz coils. The angle-resolved photoelectrons were detected normal to the sample surface and energetically analyzed by a commercial 50-mm hemispherical analyzer equipped with a low-energy spin polarization detector.[17] The overall (monochromator and spectrometer) energy resolution was 600±20 meV, determined by fitting the sharp $4f_{7/2}$ spectrum from clean W(110) using previously determined line-shape parameters.[18] The spin polarization was measured in the remnant state of the films and the complicating effect of spin-orbit-induced spin polarization[14] was eliminated by averaging two sets of data with opposite magnetization directions.

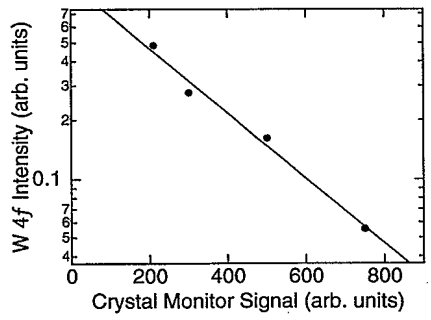

FIG. 1. W $4f$ core-level integrated photoemission intensity vs Fe film thickness. Solid circles: experiment. Solid line: exponential-decay fit to the data.

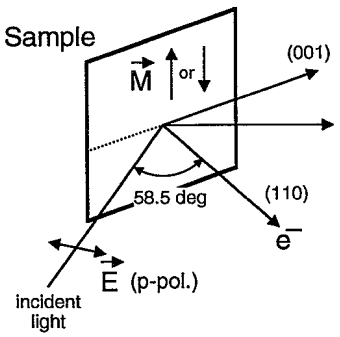

FIG. 2. Experimental geometry used in spin-polarized photoemission measurements.

III. RESULTS

Spin-resolved Fe $3p$ photoemission data from four Fe films with thicknesses of 1.4, 2.0, 3.4, and 5.1 ML have been obtained and are consecutively displayed in Figs. 3–6. In each figure (a) and (b), respectively, show the majority and minority spectra, while (c) displays the

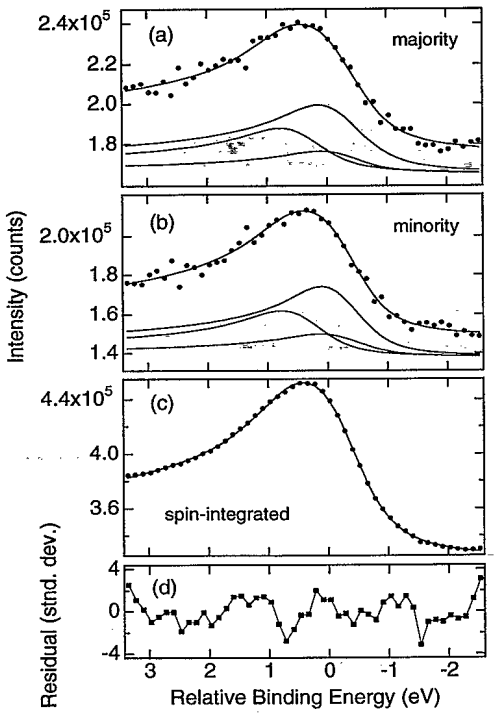

FIG. 3. Spin polarized $3p$ photoemission spectra of 1.4 ML Fe film on W(110): (a) majority spectrum, (b) minority spectrum, (c) spin-integrated spectrum, (d) residual between spin-integrated data and least-squares analysis. Solid circles: data; solid lines: least-squares analysis.

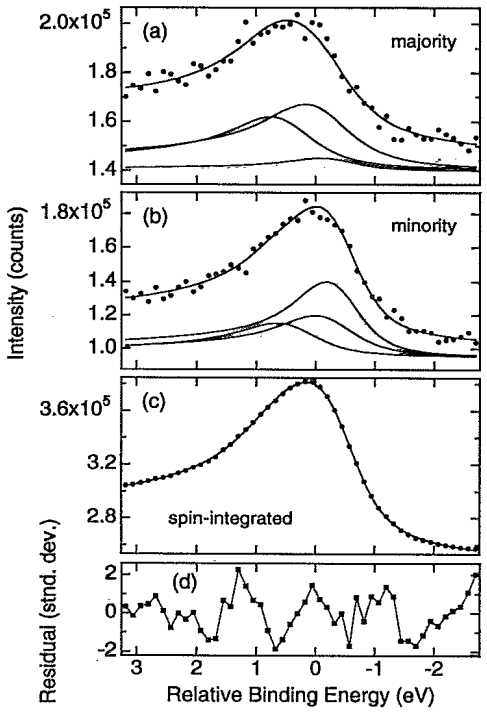

FIG. 4. Same as Fig. 3 for 2.0 ML Fe film.

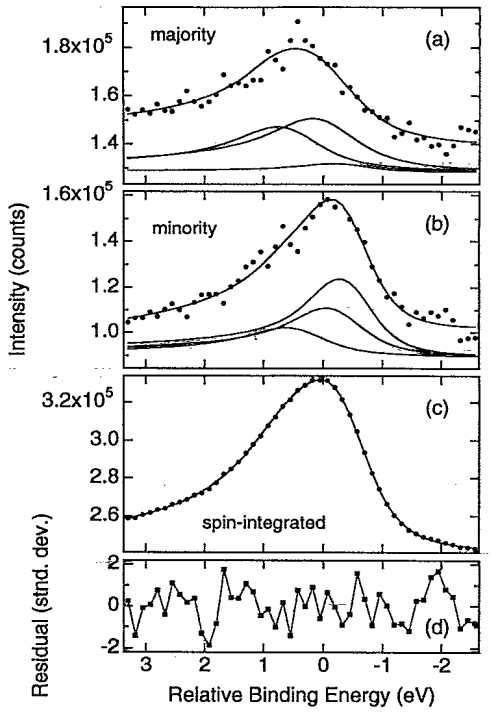

FIG. 6. Same as Fig. 3 for 5.1 ML Fe films.

spin-integrated spectrum. In agreement with previous measurements[2–6] of the $3p$ level of ferromagnetic, metallic Fe our spin-resolved spectra of the 2.0, 3.4, and 5.1 ML films exhibit a majority-spin peak with a binding energy greater than the minority-spin peak. In each of these spectra the majority peak has less weight and is broader than the minority peak. The 1.4 ML film, however, exhibits no splitting between the minority and majority peaks, and the peaks have nearly equal integrated intensities. The origin of spin-polarized splitting in these measurements is the exchange interaction between the core-hole and valence electrons. The energetic ordering observed here is consistent with an exchange interaction which energetically favors the excited core-hole shell and partially filled $3d$ valence shell to have parallel spin directions, i.e., to be ferromagnetically coupled.

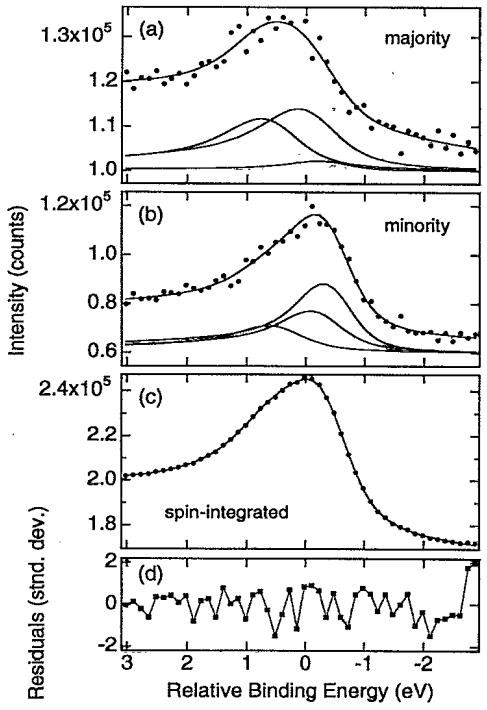

FIG. 5. Same as Fig. 3 for 3.4 ML Fe film.

IV. ANALYSIS

A. Model Hamiltonian

In order to quantitatively determine the spin-orbit interaction, exchange interaction, and line-shape parameters of our spin-resolved photoemission spectra, we introduce a simple one-particle perturbative potential $H_{\mathrm{SO+exc}}$ for the core electrons which *simultaneously* includes the spin-orbit coupling and exchange interactions:

$$H_{\mathrm{SO+exc}}=\zeta\mathbf{L}\cdot\mathbf{S}+\Delta\ . \tag{1}$$

Simultaneous treatment of the SO and exchange interactions is necessary since for the Fe $3p$ states the two interactions have nearly the same magnitude.[12] The first part of our model Hamiltonian, $\zeta\mathbf{L}\cdot\mathbf{S}$, accounts for the standard spin-orbit interaction with coupling constant ζ, orbital angular momentum $\mathbf{L}$, and spin angular momentum $\mathbf{S}$. The SO splitting $\Delta_{\mathrm{SO}}\equiv 3\zeta/2$ equals the binding-energy difference between the $p_{1/2}$ and $p_{3/2}$ peaks in the absence of any exchange interaction. The second part of the Hamiltonian Δ is a potential which couples the core-hole to the average magnetic moment of the $3d$ valence

TABLE I. Energies of photoemission components derived from model Hamiltonian.

j,m_j [a]	ΔE [b]
3/2,−3/2	$\zeta/2+\varepsilon$
3/2,−1/2	$[-\zeta+(9\zeta^2+8\zeta\varepsilon+16\varepsilon^2)^{1/2}]/4$
3/2,1/2	$[-\zeta+(9\zeta^2-8\zeta\varepsilon+16\varepsilon^2)^{1/2}]/4$
3/2,3/2	$\zeta/2-\varepsilon$
1/2,1/2	$[-\zeta-(9\zeta^2-8\zeta\varepsilon+16\varepsilon^2)^{1/2}]/4$
1/2,−1/2	$[-\zeta-(9\zeta^2+8\zeta\varepsilon+16\varepsilon^2)^{1/2}]/4$

[a]Orbital quantum numbers in the limit of zero exchange splitting.
[b]Shift in energy from state with $\zeta=\varepsilon=0$.

electrons. This type of exchange interaction, which couples the core-hole spin to the average magnetization of the valence band, is thought appropriate for itinerant ferromagnets such as Fe and has been used in previous analyses.[8,19] Its respective eigenvalues are $\pm\varepsilon$ for pure-spin, core-hole states having spin components of $\pm\hbar/2$ along the magnetization axis. The exchange splitting $\Delta_{exc}\equiv 2\varepsilon$ is the difference in binding energy between two opposite pure-spin states. In Table I we show the eigenvalues ΔE which are referenced to the energy of the six degenerate p states in the limit of $\varepsilon=\zeta=0$. Note that the j and m_j values used to identify the states in Table I are good quantum numbers only in the limit of $\varepsilon\to 0$; however, we continue to use them for nonzero ε since they are the most convenient labels for the six eigenstates and their respective eigenvalues. We note that even though our model is quite simple it produces the same angular-momentum-projected density of states as the more sophisticated calculation by Tamura *et al.*[8]

We calculate the photoemission intensities, i.e., the relative transition strengths, under the assumptions of (1) radial wave functions independent of the photoelectron orbital state, (2) no interference between photoelectron states with different angular momenta l' and m', and (3) no photoelectron diffraction. (We thus cannot account for spin-orbit induced spin polarization of the photoelectron spectra.[14]) With these assumptions the transition strength for a core-hole state $\psi_i(\mathbf{r})$, obtained via the Fermi golden rule in the dipole approximation, is proportional to

$$\sum_{l'm'} Y^2_{l'm'}(\theta_k,\phi_k)|\langle Y_{l'm'}|\,\mathbf{A}\cdot\mathbf{r}|\psi_i\rangle|^2\,, \qquad (2)$$

where $\mathbf{A}$ is the vector potential and θ_k and ϕ_k are the polar and the azimuthal angles in which photoelectrons are emitted.[20] From Eq. (2) it is obvious that in general the intensity depends upon the incident-light direction and polarization, the photoelectron emission direction, and the outgoing-electron spin polarization. For a p-state core hole the dipole approximation produces intensity only in s and d outgoing states. Calculated spin-resolved intensities of the six p-level eigenstates for angle-averaged photoemission are presented in Table II. Intensities for $\Delta_{exc}=0.4$ eV and $\Delta_{SO}=0.75$ eV are further illustrated in Fig. 7. The top and bottom parts of the figure show p to s and p to d transitions, respectively.

TABLE II. Calculated component intensities for angle-integrated, spin-resolved photoemission for $p\to s$ and $p\to d$ transitions

j,m_j [a]	Relative transition strengths[b,c] Majority $p\to s$	Majority $p\to d$	Minority $p\to s$	Minority $p\to d$
3/2,−3/2	0	0	1	1
3/2,−1/2	λ_2	λ_2	0	$(6/7)(1-\lambda_2)$
3/2,1/2	0	$(6/7)(1-\lambda_1)$	λ_1	λ_1
3/2,3/2	1	1	0	0
1/2,1/2	0	$(6/7)(1-\lambda_4)$	λ_4	λ_4
1/2,−1/2	λ_3	λ_3	0	$(6/7)(1-\lambda_3)$

[a]Orbital quantum numbers in the limit of zero exchange splitting.
[b]The values of λ_i are as follows:

$\lambda_1=(1+a^2)^{-1}, a=[\zeta-4\varepsilon+(9\zeta^2-8\zeta\varepsilon+16\varepsilon^2)^{1/2}]/(2\sqrt{2}\zeta)$.

$\lambda_2=b^2/(1+b^2), b=[-\zeta-4\varepsilon+(9\zeta^2+8\zeta\varepsilon+16\varepsilon^2)^{1/2}]/(2\sqrt{2}\zeta)$,

$\lambda_3=c^2/(1+c^2), c=[-\zeta-4\varepsilon-(9\zeta^2+8\zeta\varepsilon+16\varepsilon^2)^{1/2}]/(2\sqrt{2}\zeta)$,

$\lambda_4=(1+d^2)^{-1}, d=[\zeta-4\varepsilon-(9\zeta^2-8\zeta\varepsilon+16\varepsilon^2)^{1/2}]/(2\sqrt{2}\zeta)$.

[c]The maximum transition strength for $p\to s$ or $p\to d$ emission is normalized to 1.

A comparison of Fig. 7 with the present and previously published 2p and 3p spin-polarized core-level spectra from itinerant ferromagnets such as Fe (Refs. 2–6 and 21) and Co (Refs. 22 and 23) shows that the model quali-

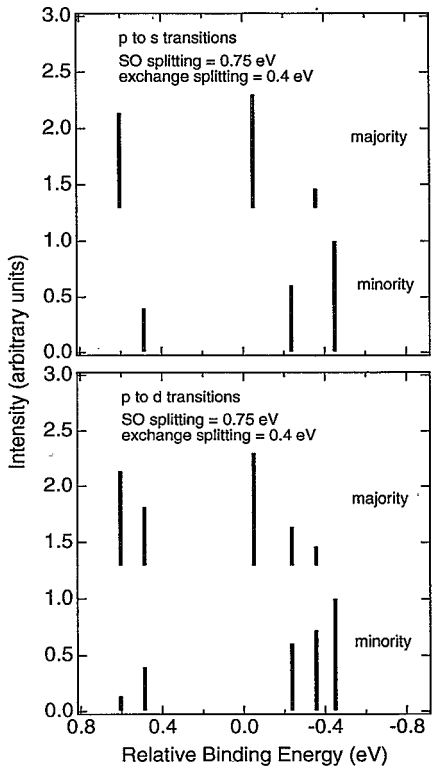

FIG. 7. Calculated intensities of p states in spin-resolved photoemission for angle-integrated p to s and p to d transitions.

tatively describes the observed features. For $2p$ photoemission, where the $p_{3/2}$ and $p_{1/2}$ manifolds largely maintain their integrity, our model predicts the $p_{3/2}$ minority emission to be more intense and at lower binding energy than its majority counterpart. In contrast the $p_{1/2}$ emission has more intensity in the higher-binding-energy majority channel. Both of these features are experimentally observed.[2,21,23] For $3p$ photoemission, where the SO interaction, exchange interactions, and lifetime broadening are all approximately the same size, the model predicts a more sharply peaked minority spectrum with an overall shift to lower binding energy when compared to the majority spectrum, in agreement with our measurements (Figs. 4–6) and previous observations.[2–6,22]

B. Application to Fe 2p MCD photoemission

As a quantitative test of our model to simultaneously describe the spin-orbit and exchange interactions of a core hole we first apply the model to recent Fe $2p$ magnetic circular dichroism (MCD) photoemission data of Baumgarten *et al.*[13] In MCD photoemission, separate spectra are collected with the photon helicity (right-hand circularly polarized or left-hand circularly polarized) parallel and antiparallel to the sample magnetization. The data are reported as an intensity asymmetry $[(I^+-I^-)/(I^++I^-)]$ between the intensities I^+ and I^- collected for the parallel and antiparallel conditions, respectively. In Fig. 8(b) we show the MCD asymmetry data of Baumgarten *et al.* as the filled circles with the error bars.

In fitting the asymmetry data we fixed the background intensity and the overall $2p_{3/2}$ peak height to match the experimental I^+ and I^- data. Each core-level component[24] is modeled by a Doniach-Šunjić (DS) function[25] convolved with a Gaussian (to represent the instrumental broadening).[26] The shape of the DS function is determined by two parameters, the Lorentzian lifetime full-width half-maximum Γ and a singularity index α which describes the asymmetry of the line. The Lorentzian widths were fixed at 0.80 and 1.25 eV for the $2p_{3/2}$ and $2p_{1/2}$ lines, respectively.[27] The singularity index α was set to 0.27 (as determined below for thick Fe films), while the Gaussian contribution was left as a free parameter. Since in the experiment the kinetic energy of the outgoing photoelectrons is rather high at $\sim$150 eV, the photoelectron d channel is expected to dominate the s channel;[28] hence, we neglect the s states in this comparison. Additionally, the SO splitting $3\zeta/2$ is held to 13.0 eV, the observed separation between the spin-integrated $p_{3/2}$ and $p_{1/2}$ peaks.[13,21]

Under these specific assumptions (and the more general ones noted above) our model predicts the normalized intensities shown in Table III for the corresponding eigenenergies listed in Table I. With these constraints a nonlinear least-squares fit produces the solid line through the data in part (b) of Fig. 8. Our model clearly reproduces all of the features of the MCD asymmetry spectrum. From the fit we extract an exchange splitting $\Delta_{exc}=0.90\pm0.05$ eV. This value is quite close to the theoretical result of $\Delta_{exc}=0.8$ eV by Ebert.[12] In (a) of Fig. 8 we show the two helicity-resolved intensities, I^+ and I^-, calculated from the model. The splittings are 0.43 and 0.18 eV for the $p_{3/2}$ and $p_{1/2}$ peaks, respectively. These are in good agreement with the experimental splittings of 0.5 ± 0.2 and 0.3 ± 0.2 eV.[13] The model thus appears quite capable of representing core-level photoemission spectra of ferromagnetic, metallic Fe. We note that the MCD splitting of either the $p_{3/2}$ or $p_{1/2}$ peaks significantly underestimates the exchange splitting Δ_{exc}.

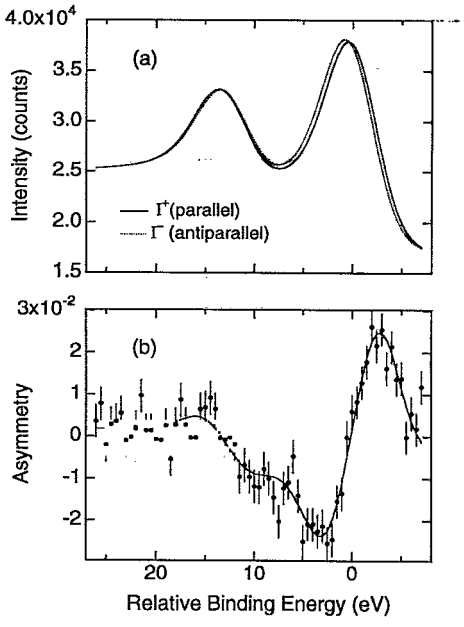

FIG. 8. Least-squares analysis of Fe $2p$ MCD asymmetry data (Ref. 12). (a) calculated I^+ and I^- intensities. (b) MCD data (solid circles with error bars) and least-squares fit (solid line).

C. Spin-polarized Fe 3p photoemission

We now apply our model to the thin-film Fe data shown in Figs. 3–6 in order to extract the spin-orbit splitting, exchange splitting, and line-shape parameters for each set of data. For photoelectron kinetic energies

TABLE III. Calculated component intensities in MCD photoemission for experimental geometry of Baumgarten *et al.* (Ref. 13).

j,m_j[a]	Relative transitions strengths[b] I^+ spectrum	I^- spectrum
3/2,−3/2	1/6	1
3/2,−1/2	$(3-2\lambda_2)/6$	$(1+\lambda_2)/2$
3/2,1/2	$(1+\lambda_1)/2$	$(3-2\lambda_1)/6$
3/2,3/2	1	1/6
1/2,1/2	$(1+\lambda_4)/2$	$(3-2\lambda_4)/6$
1/2,−1/2	$(3-2\lambda_3)/6$	$(1+\lambda_3)/2$

[a]Orbital quantum numbers in the limit of zero exchange splitting.

[b]The values of λ_i are given in Table II.

TABLE IV. Results from analysis of Fe 3p spin-polarized data for epitaxial Fe films on W(110).

Fe film thickness (ML±20%)	1.4	2.0	3.4	5.1
Background polarization (%)	7±1.5	16±2	19±2.5	19±3
SO splitting (eV)	0.66±0.02	0.67±0.04	0.69±0.04	0.66±0.05
Exchange splitting (eV)	0.0±0.12	0.29±0.05	0.42±0.04	0.41±0.05
Singularity index	0.45±0.01	0.32±0.01	0.26±0.01	0.27±0.01
$\Gamma_\uparrow$ (eV)	0.94±0.26	1.17±0.08	1.01±0.07	1.22±0.08
$\Gamma_\downarrow$ (eV)	0.87±0.25	0.74±0.05	0.60±0.03	0.75±0.04
$\Gamma_\uparrow/\Gamma_\downarrow$	1.08±0.44	1.58±0.15	1.68±0.16	1.63±0.14
$I_\downarrow/I_\uparrow$	1.01±0.27	1.50±0.28	1.77±0.28	1.37±0.24

applicable to our experiment (~40 eV),[29] calculations[28] for 3p photoemission from nearby elements (Ni, Cu, Ga, and Ge) indicates that the d-wave to s-wave intensity ratio is of the order of 1:1. However, for our experimental geometry of normal emission the s and d wave intensities are proportional. Hence, in what follows, we consider only p to s transitions (see Table II) in the data analysis. Note that the theoretical model predicts overall equal intensities in the majority and minority spectra.

Each data set was analyzed by a simultaneous nonlinear least-squares fitting of the spin-integrated and spin-resolved spectra. In analyzing the data the Gaussian width was set equal to the experimental resolution of 600 meV. Two different Lorentzian-width parameters were used, one for a pure spin-up core hole ($\Gamma_\uparrow$) and one for a pure spin-down core hole ($\Gamma_\downarrow$). For simplicity, the Lorentzian width for each of the six components is set to $A\Gamma_\uparrow + B\Gamma_\downarrow$ where A and B are the probabilities of the eigenstate being spin up or spin down, respectively. The singularity index parameter α was constrained to be the same for all components. A minority/majority scaling parameter $I_\downarrow/I_\uparrow$, which is not inherent in the model, was introduced in order to account for the experimental observation that the overall intensity of the minority and majority spectra are unequal. This is discussed in more detail below.

In Figs. 3–6 the lines which pass through the data are the fitted majority, minority, and spin-integrated intensities in parts (a), (b), and (c), respectively. The solid lines below the data in (a) and (b) show the six fitting components (intensities listed in Table II) for the spectra. The statistical nature of the residuals (for the spin-integrated spectrum), shown in (d) of the figures, demonstrates that our one-particle model fully accounts for the Fe 3p spin-resolved photoemission features.

The results of the least-squares analysis, summarized in Table IV, show several obvious trends as the film thickness is increased. The background polarization increases by a factor of ~2.5 from 1.4 to 5.1 ML. The exchange splitting also markedly increases with increasing thickness, from 0.0±0.12 eV for 1.4 ML to 0.41±0.05 eV for the 5.1 ML film. Within errors, the SO splitting remains constant with increasing film thickness as expected for Fe atoms in very similar metallic environments. The SO splitting is quite well described by a value of 0.67±0.02 for all four film thicknesses. With increasing film thickness the singularity index decreases from 0.45±0.01 to 0.27±0.01. The data also shows a $\Gamma_\uparrow$ to $\Gamma_\downarrow$ ratio of ~1.6 for the three thickest films.

In fitting the data we have not included any interface-atom core-level shifts (ICS's) or surface-atom core-level shifts (SCS's) of the core-electron binding energies.[30] The excellent fits to the four data sets suggest that such shifts are indeed negligible on the scale of the exchange or spin-orbit splittings. Theoretical calculations for the SCS's of Fe support this conclusion for the surface atoms: the SCS has been calculated to be <50 meV using two different theories.[31,32] The small SCS for Fe suggests that the core-level binding energies for metallic Fe atoms are rather insensitive to the chemical environment. Hence, we expect the ICS to be similarly small and thus insignificant in our analysis. In fact, since by gross measures the electronic structures of W and Fe are quite similar [electronegativity difference of 0.1 (Ref. 33) and first-ionization-energy difference of 0.12 eV (Ref. 34)] one expects the ICS to be even smaller in magnitude than the SCS since the environment of a bulk atom is expected to be closer to an interface Fe atom than to a surface Fe atom.

V. DISCUSSION

The magnetization of the films is directly related to the secondary-electron polarization (SEP). Previous measurements have shown that the SEP of bulk Fe drops from a value of 45% near 5 eV kinetic energy to ~27% at 10 eV.[29,35] Between 10 and ~25 eV the polarization remains constant at ~27%, a value equal to the 3d valence-electron polarization.[35] Such a plateau in SEP at the valence-band polarization is expected theoretically[36] and has been observed in several 3d ferromagnetic systems.[35–38] At higher kinetic energies, in $Fe_{83}B_{17}$, e.g.,[38] the SEP has been observed to smoothly decrease from the plateau valence-band polarization level to zero with increasing kinetic energy towards the primary excitation energy.

Our measured SEP's have implications for the intrinsic SEP of bulk Fe at a kinetic energy of 40 eV. The measured polarizations are not equal to the intrinsic SEP of the Fe films since there is an unpolarized contribution from the W substrate which is responsible, in part, for the decrease in measured SEP with decreasing film thickness. In Fig. 9 we plot the measured polarizations (solid circles with error bars) and several calculations of the

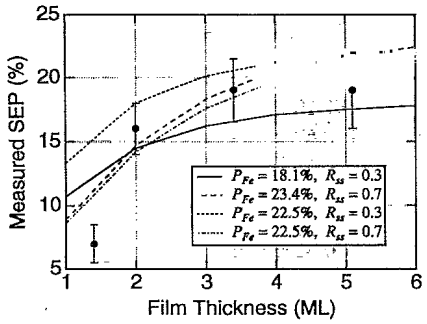

FIG. 9. Measured secondary electron polarization vs Fe film thickness. Data are the solid circles with error bars and calculations with shown parameters are the various lines.

measured polarization vs film thickness. The calculations are based on a model which assumes that an unpolarized contribution arises from the secondary spectrum of the W substrate and that this unpolarized component is attenuated by the Fe film in escaping from the sample. In the model there are two parameters in addition to the IMFP in the Fe films. The first is the intrinsic secondary-spectrum-strength ratio R_{ss} between W and Fe for photoexcitation at 93 eV. From calculations of the photoionization cross sections of Fe and W electronic states[39] with binding energies lower than the Fe $3p$ level, we estimate this ratio to be ~ 0.5. The second parameter is the intrinsic SEP of bulk Fe, P_{Fe}, at 50 eV. We have determined the possible range of P_{Fe} based upon the conclusion that the two thickest films have an inherent SEP equal to bulk Fe. (This conclusion comes from the observations that the two thickest films display identical secondary-electron polarizations, exchange splittings, and singularity indices which imply they have essentially the band structure, and hence the intrinsic SEP spectrum, of bulk Fe.) With this assumption and an estimate of $R_{ss}=0.5\pm0.2$, the solid and dashed lines in Fig. 9 maximize the range of possible P_{Fe} values. From this we conclude that $P_{Fe}=20.8\pm2.7\%$. This is somewhat smaller than the bulk polarization of 27%, indicating that 40 eV kinetic energy is slightly above the SEP plateau region. However, since this SEP is fairly close to the plateau value of 27%, in what follows we assume that the 40 eV intrinsic SEP is proportional to the magnetic moment per atom of the films.

Our measured SEP's also put constraints on the magnetic moment of the thinnest (1.4 ML) Fe film. As discussed above, a diminished polarization with decreasing film thickness arises from unpolarized secondary-electron emission from the W substrate; however, this effect cannot account for all of the decrease observed in the thinnest film. The dotted and dot-dashed curves in Fig. 9 maximize the possible range of calculated polarizations at 1.4 ML consistent with the above assumptions and an additional assumption that the 2.0-ML-film intrinsic polarization is less than or equal to the polarization of the two thickest films. (This last assumption is based on the observation that the exchange splitting for this film is between the 1.4-ML and thick film values.) Neither calculated curves shows as large a reduction in polarization as measured: we deduce a calculated polarization at 1.4 ML of $13\pm2\%$, significantly greater than the experimental value of $7\pm1.5\%$. Hence, the thinnest film appears to have a magnetic moment per Fe atom of only $1.2\pm0.3\mu_B$ compared to the bulk Fe value of $2.22\mu_B$. Theoretically, for 1 ML of Fe on W(110) a slightly reduced moment of $2.18\mu_B$ has been predicted.[40]

Even though the thinnest film has a reduced moment compared to bulk Fe,[41] the exchange splitting of its $3p$ spectra is surprisingly small, 0 ± 0.12 eV. The resulting reduced degree of complication in the spectra allows us to take with confidence the 1.4-ML film SO splitting of 0.66 ± 0.02 eV. This SO splitting value in turn provides a test for the analysis of the thicker films where the exchange splitting is significant. It is satisfying to see that the SO splitting for all four films is, within errors, identical. We can thus further take with confidence the deduced exchange splittings.

In Fig. 10 we plot the fitted exchange splittings vs the magnetic moment of the films (deduced from Fig. 9 assuming that the intrinsic SEP is proportional to the moment). We have used the above conclusion that the two thickest films have a moment equal to bulk Fe and have averaged their results for the exchange splitting. Although both the moment and Δ_{exc} increase with film thickness, the relationship is clearly not proportional. Such nonproportionality between the core-hole–valence-band exchange interaction and the magnetic moment has been previously pointed out by van Acker *et al.* in analysis of Fe $3s$ spectra.[42]

The deduced exchange splitting for the two thickest films is approximately 33% smaller than that merely obtained from the separation in peak positions. E.g., the curves fitted to the minority and majority spectra for 5.1 ML show a peak separation of 0.61 eV even though $\Delta_{exc}=0.40\pm0.05$ eV. The reason for this becomes apparent from inspection of the spectra and the fitting components (Figs. 5 and 6 for the two thickest films). Since Δ_{exc} is defined as the binding-energy difference between pure spin-up and spin-down states (with other quantum numbers equivalent), Δ_{exc} is given by the energy difference between the largest components in the minority and majority analysis which are the pure-spin $m_j=3/2$ and $m_j=-3/2$ states, respectively. The

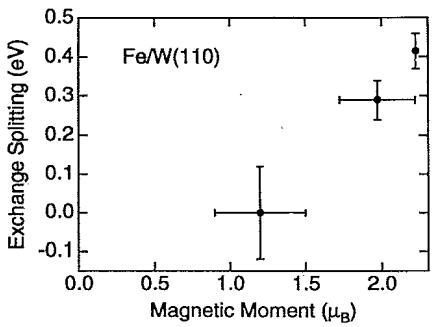

FIG. 10. Exchange splitting Δ_{exc} vs magnetic moment of Fe films.

analysis clearly shows, however, that the peaks in minority and majority intensities are separated by a greater amount due to the relatively large spectral weight of the $j=1/2$ component in the majority spectra. Our peak separation of 0.61 eV for the 5.1 ML film lies half way between previously measured spin-resolved peak separations of 0.5 (Refs. 4 and 5) and 0.7 eV.[6] However, since the component intensities are dependent upon the experimental geometry and incident-light polarization, these numbers are not necessarily directly comparable.

Our spin-orbit splitting of 0.67 ± 0.02 eV is in excellent agreement with the value of 0.7 eV deduced from peak separations in spin-resolved MLD spectra in which the spin-orbit interaction (instead of the exchange interaction) was the cause of the spin polarization.[10] These results for Δ_{SO} and our exchange splitting of 0.41 ± 0.05 eV are both smaller than the values of $\Delta_{SO}=1.1\pm0.1$ and $\Delta_{exc}=0.95\pm0.05$ recently obtained by Tamura *et al.* in analysis of spin-integrated MLD and MCD spectra.[8] We suggest that the difference arises from their neglect of the singularity index which substantially broadens the (experimental) spectra compared to (calculated) spectra without its inclusion. Indeed, using our model to fit their MCD spectra from 2 ML of Fe/Cu(100) (Fig. 3 in Ref. 8), we obtain $\Delta_{SO}=0.64\pm0.05$ and $\Delta_{exc}=0.09\pm0.08$, consistent with the values deduced from our films.

With increasing film thickness the singularity index decreases substantially from 0.45 ± 0.01 to 0.27 ± 0.01. The value of 0.27 ± 0.01 is identical to that obtained from spin-integrated Fe 3s photoexcitation.[42] In other metals systematic differences in α have been attributed to differences in the relative amount of s (vs higher orbital-momentum character) screening charge. E.g., in the transition metals W (Ref. 18) and Ta (Ref. 43) and in the alkali metals[44] the larger α for surface atoms appears due to the more atomiclike nature of the surface atoms which is characterized a higher degree of s charge in the valence band. Since atomic Fe is also characterized by more valence s charge than bulk Fe, we suggest that as the films become thicker the overall electronic structure becomes less atomiclike and more bulklike, resulting in the measured decrease in α.

Recently Van Campen, Pouliot, and Klebanoff[2] have fit spin-resolved Fe 3p photoexcitation spectra with different α's for majority-spin and minority-spin electrons and obtained a slightly larger singularity index for the majority-spin spectrum, $\alpha_{maj}=0.39\pm0.02$ and $\alpha_{min}=0.35\pm0.02$. However, their fitting did not account for the spin-orbit interaction. Their larger deduced α's and spin-resolved difference in α are likely due to neglect of the $j=\frac{1}{2}$ components in the spectra. Our analysis indicates no appreciable difference in α for the different spin-resolved states.

The extracted Lorentzian widths for the two thickest films, average values of $\Gamma_\uparrow=1.1\pm0.2$ eV and $\Gamma_\downarrow=0.7\pm0.1$ eV, are substantially smaller than previously reported values.[2,3] Again, this can be ascribed to past neglect of the SO splitting which necessarily resulted in the Lorentzian width compensating for the SO-splitting induced broadening of the spectra. For all of the films, the ratio of $\Gamma_\uparrow$ to $\Gamma_\downarrow$ is greater than 1 and appears to increase with the magnetic moment of the films. In the past the ratio has been intuitively explained by a simple argument that the core-hole lifetime is proportional to the number of available valence electrons to fill the core-hole by a non-spin-flip core-valence-valence Auger transition. Figure 11, which plots the lifetime ratio vs the majority to minority electrons ratio $N_\uparrow/N_\downarrow$ in the occupied 3d band (calculated from the SEP-deduced magnetic moments in Fig. 10) shows a relationship consistent with a proportionality constant of 1 (fitted value of 0.95 ± 0.05), in agreement with this intuitive idea.

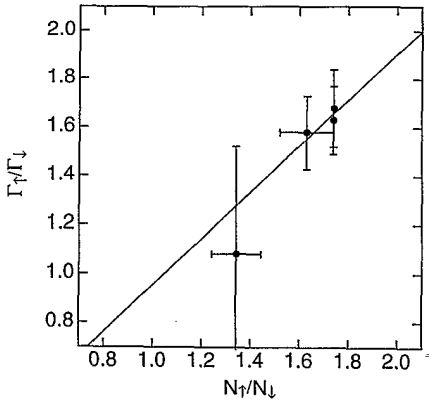

FIG. 11. Lifetime-width ratio for spin-up and spin-down core holes vs occupation-level ratio of Fe 3d valence band. Straight line is a proportional fit to the data (solid circles with error bars).

The one feature of the experimental spectra not accounted for by our one-electron model is the relative spectral weight of the majority and minority peaks. As for any theory which simply couples the spin of the core hole to the average spin of the valence band (and neglects final-state scattering effects), the predicted ratio is unity. While data from the thinnest film is consistent with this ratio, the three thickest films all have a ratio $I_\downarrow/I_\uparrow\approx1.5$. In other studies of the Fe 3p level intensity ratios of 1,[3] 1.25,[2] 1.3–1.4,[4] and 2.6 (Ref. 6) have been observed with photon energies of 92, 1254, 90, and 250 eV, respectively. In all cases the majority intensity is smaller than (or equal to) the minority intensity.

Final-state effects such as spin-dependent diffraction or a spin-dependent IMFP seem to be ruled out as an explanation. The fact that $I_\downarrow/I_\uparrow$ is consistently greater than 1 immediately suggests a spin-dependent IMFP. However, data obtained at 38 eV kinetic energy show that the IMFP's for spin-up and spin-down electrons are nearly identical.[16] Recently Tamura *et al.* have suggested that multiple scattering plays an important role in describing spin-sensitive photoexcitation from the Fe 3p level.[8] However, if diffraction were a major contributor to $I_\downarrow/I_\uparrow$ then one would expect at some photon energies that $I_\downarrow I_\uparrow$ would be less than 1. Another area our model has neglected is the interference between states of the photoemitted electron. However, as in the case of diffraction, it is not clear how this would always manifest itself as an increase in the minority intensity.

This lack of explanation of $I_\downarrow/I_\uparrow$ in approximations of

the photoexcitation final state suggests that the nonunity intensity ratio lies in the approximate description of the core-hole–valence-band interaction. I.e., the itinerant description of Fe ferromagnetism is not quite valid and that to fully explain the core-hole–valence-band interaction one must describe the eigenstates more realistically. Our observed value of $I_\downarrow/I_\uparrow=1.01\pm0.27$ for $\Delta_{exc}=0.0\pm0.12$ in the thinnest film supports this conjecture. We suggest, however, based upon the excellent, internally consistent fits to the data presented here, that the correct description is not substantially different from our model and that its main effect is to alter the spin-up–spin-down intensity ratio. Clearly, data at a substantially improved resolution will be crucial in sorting out this issue.

VI. CONCLUSIONS

The most important conclusion to emerge from this study is that a proper interpretation of spin-sensitive photoexcitation spectra critically requires a realistic model. In the case of the Fe $3p$ spectrum inclusion of the spin-orbit splitting is crucial for meaningful extraction of other spectral parameters. Our analysis suggests that previous neglect of the SO coupling resulted in singularity index and lifetime values which were overestimated. Our analysis has further shown that the majority-electron–minority-electron peak separation in spin-resolved photoexcitation or the peak separations in MCD photoexcitation are often rather poor estimates of the exchange interactions.

ACKNOWLEDGMENTS

The authors gratefully acknowledge the assistance of K. Garrison and Q. Y. Dong in this effort and would like to thank L. Kleinman for valuable suggestions. D.-J. H. acknowledges stimulating conversations with P. D. Johnson. This work was supported by National Science Foundation under Grant No. DMR93-03091. The National Synchrotron Light Source is supported by the U.S. Department of Energy.

*Present address: Physics Department, Brookhaven National Laboratory, Upton, NY 11973.

[1]C. S. Fadley, D. A. Shirley, A. J. Freeman, and J. V. Mallow, Phys. Rev. Lett. **23**, 1397 (1969).

[2]D. G. Van Campen, R. J. Pouliot, and L. E. Klebanoff, Phys. Rev. B **48**, 17 533 (1993).

[3]C. Carbone and E. Kisker, Solid State Commun. **65**, 1107 (1988).

[4]B. Sinkovic, P. D. Johnson, N. B. Brookes, A. Clarke, and N. V. Smith, Phys. Rev. Lett. **65**, 1647 (1990).

[5]G. A. Mulhollan, A. B. Andrews, and J. L. Erskine, Phys. Rev. B **46**, 11 212 (1992).

[6]R. Jungblut, Ch. Roth, F. U. Hillebrecht, and E. Kisker, Surf. Sci. **269/270**, 615 (1992).

[7]F. Sirotti, M. De Santis, and G. R. Rossi, Phys. Rev. B **48**, 8299 (1993).

[8]E. Tamura, G. D. Waddill, J. G. Tobin, and P. A. Sterne, Phys. Rev. Lett. **73**, 1533 (1994).

[9]G. Rossi, F. Sirotti, N. A. Cherepkov, F. C. Farnoux, and G. Panaccione, Solid State Commun. **90**, 557 (1994).

[10]Ch. Roth, F. U. Hillebrecht, H. B. Rose, and E. Kisker, Phys. Rev. Lett. **70**, 3479 (1993).

[11]A majority (minority) core hole is defined as a core hole left behind by a majority (minority) photoelectron. However, a majority or minority core hole is not necessarily in a pure-spin state. A majority (minority) photoelectron is one whose magnetic moment is parallel (antiparallel) with the magnetization of the sample.

[12]H. Ebert, J. Phys. Condens. Matter **1**, 9111 (1989).

[13]L. Baumgarten, C. M. Schneider, H. Petersen, F. Schafers, and J. Kirschner, Phys. Rev. Lett. **65**, 492 (1990).

[14]Spin-orbit splitting of the core-hole and spin-orbit-induced spin polarization of the photoemission spectra are two different effects and should not be confused. The former arises from the coupling of the spin and orbital angular momentum degrees of freedom of the excited core-level shell, while the latter effect arises from interference between the $l+1$ and $l-1$ states of the photoemitted electron. [See, e.g., Ch. Roth, F. U. Hillebrecht, W. G. Park, H. B. Rose, and E. Kisker, Phys. Rev. Lett. **73**, 1963 (1994).]

[15]P. J. Berlowitz, J.-W. He, and D. W. Goodman, Surf. Sci. **231**, 315 (1990).

[16]D. P. Pappas *et al.*, Phys. Rev. Lett. **66**, 504 (1991).

[17]M. R. Scheinfein, D. T. Pierce, J. Unguris, J. J. McClelland, R. J. Celotta, and M. H. Kelley, Rev. Sci. Instrum. **60**, 1 (1989).

[18]D. M. Riffe, G. K. Wertheim, and P. H. Citrin, Phys. Rev. Lett. **63**, 1976 (1989).

[19]H. Ebert, L. Baumgarten, C. M. Schneider, and J. Kirschner, Phys. Rev. B **44**, 4406 (1991).

[20]S. M. Goldberg, C. S. Fadley, and S. Kono, J. Electron Spectrosc. Relat. Phenom. **21**, 285 (1981).

[21]B. Sinkovic and E. Shekel, in *BNL National Synchrotron Light Source Activity Report 1993*, edited by E. Z. Rothman (Brookhaven National Laboratory, Upton, New York, 1994), p. 48.

[22]W. Clemens, E. Vescovo, T. Kachel, C. Carbone, and W. Eberhardt, Phys. Rev. B **46**, 4198 (1992).

[23]L. E. Klebanoff, D. G. Van Campen, and R. J. Pouliot, Phys. Rev. B **49**, 2047 (1994).

[24]Here and throughout the paper we use peak to refer to an observed spectral feature in the spectra. We use component to refer to a photoemission state arising from an eigenstate of the core-excited solid which may or may not be resolved in the spectra.

[25]S. Doniach and M. Šunjić, J. Phys. C **3**, 285 (1970).

[26]While, in principle, phonon broadening also contributes to the Gaussian width, its contribution for Fe is predicted to be negligible; see C. P. Flynn, Phys. Rev. Lett. **37**, 1445 (1976).

[27]J. C. Fuggle and S. F. Alvarado, Phys. Rev. A **22**, 1615 (1980).

[28]S. M. Goldberg, C. S. Fadley, and S. Kono, J. Electron Spectrosc. Relat. Phenom. **26**, 285 (1981).

[29]The kinetic energy of the electron is referenced to the Fermi energy of the sample.

[30]The SCS is defined to be the surface-atom binding energy minus the bulk-atom binding energy. The ICS is similarly

defined for Fe atoms sitting on the W(110) surface.
[31]D. Tomanek, V. Kumar, S. Holloway, and K. H. Bennemann, Solid State Commun. **41**, 273 (1982).
[32]P. H. Citrin and G. K. Wertheim, Phys. Rev. B **27**, 3176 (1983).
[33]L. Pauling, *General Chemistry* (Dover, New York, 1988), p. 192.
[34]L. Pauling, *General Chemistry* (Ref. 33), p. 118.
[35]E. Kisker, W. Gudat, and K. Schröder, Solid State Commun. **44**, 591 (1982).
[36]D. R. Penn, S. P. Apell, and S. M. Girvin, Phys. Rev. Lett. **55**, 518 (1985); Phys. Rev. B **32**, 7753 (1985).
[37]H. Hopster, R. Raue, E. Kisker, G. Güntherodt, and M. Campagna, Phys. Rev. Lett. **50**, 70 (1982).
[38]M. Landolt and D. Mauri, Phys. Rev. Lett. **49**, 1783 (1982).
[39]J. J. Yeh and I. Lindau, At. Data Nucl. Data Tables **32**, 1 (1985).
[40]S. C. Hong, A. J. Freeman, and C. L. Fu, Phys. Rev. B **38**, 12 156 (1988).
[41]That thin films (>0.8 ML) of Fe on W(110) are ferromagnetic has also been observed in Kerr-effect measurements [Araya-Pochet, G. A. Mulhollan, and J. L. Erskine (unpublished)] and in spin-polarized electron diffraction [H. J. Elmers *et al.*, Phys. Rev. Lett. **73**, 898 (1994)].
[42]J. F. van Acker, Z. M. Stadnik, J. C. Fuggle, H. J. W. Koekstra, K. H. Buschow, and G. Stroink, Phys. Rev. B **37**, 6827 (1988).
[43]D. M. Riffe, W. Hale, B. Kim, and J. L. Erskine, Phys. Rev. B **51**, 11 012 (1995).
[44]G. K. Wertheim, D. M. Riffe, and P. H. Citrin, Phys. Rev. B **45**, 8703 (1992).